

1 Cellular tolerance at the  $\mu$ -opioid receptor is phosphorylation dependent

2

3 Seksiri Arttamangkul, Daniel A Heinz, James R Bunzow, Xianqiang Song & John

4 T Williams\*

5 The Vollum Institute, Oregon Health & Science University, 3181 SW Sam Jackson

6 Park Rd, Portland, OR 97239

7

8 Corresponding Author:

9 John T Williams

10 Vollum Institute, OHSU

11 3181 SW Sam Jackson Park Rd

12 Portland, OR 97239

13

13

14 **Abstract**

15 The role of phosphorylation of the  $\mu$ -opioid receptor (MOR) in desensitization,  
16 internalization and long-term tolerance was examined in locus coeruleus (LC)  
17 neurons. Viral expression of wild type (exWT) and mutant MORs, where all  
18 phosphorylation sites on the C-terminus (Total Phosphorylation Deficient (TPD))  
19 were mutated to alanine, were examined in a MOR knockout rat. Both expressed  
20 receptors acutely activate potassium conductance similar to endogenous  
21 receptors in wild type animals. The exWT receptors, like endogenous receptors,  
22 displayed signs of tolerance after chronic morphine treatment. There was  
23 however a loss of agonist-induced desensitization and internalization in  
24 experiments with the TPD receptors. In addition the development of tolerance  
25 was not observed in the TPD receptors following chronic morphine treatment.  
26 The results indicate a key role of C-terminal phosphorylation in the expression of  
27 acute desensitization, trafficking and long-term tolerance to morphine.

28

29 **Introduction**

30 Considerable effort has been aimed at characterizing the mechanisms that  
31 underlie acute  $\mu$ -opioid receptor (MOR) dependent desensitization and cellular  
32 tolerance (Williams et al., 2013). One key step thought to be important in these  
33 processes is the phosphorylation of sites on the cytoplasmic loops and C-terminal  
34 tail following receptor activation. On the C-terminal tail of the MOR there are 11  
35 possible phosphorylation sites. Two specific cassettes, amino acid residues 354 to  
36 357 (TSST) and 375 to 379 (STANT), are phosphorylated following application of  
37 agonists that induce desensitization and internalization (Lau et al., 2011). Point  
38 mutations of serine (S) and threonine (T) residues in the STANT sequence  
39 resulted in a decrease in agonist induced arrestin recruitment and  
40 internalization, but do not eliminate the induction of acute desensitization (Lau  
41 et al., 2011; Birdsong et al., 2015). Complete alanine mutation of both the TSST  
42 and STANT sequences significantly reduced, but did not completely eliminate

43 acute desensitization. Although the TSST and STANT sequences are known to be  
44 agonist-dependent phosphorylation sites, there are four other serine and  
45 threonine sites on the C-terminus that are either phosphorylated constitutively or  
46 by agonist dependent kinases (Williams et al., 2013). It is not known if  
47 phosphorylation of these sites alters the regulation of MORs.

48

49 The present study investigated the role of C-terminus MOR phosphorylation on  
50 acute signaling, desensitization, internalization and cellular tolerance in rats. The  
51 desensitization of MOR in rat locus coeruleus neurons has been studied  
52 extensively in wild type animals. In order to study wild type and mutant MORs, a  
53 MOR-knockout rat model was used and MORs were virally expressed. Studying  
54 receptor trafficking of expressed receptors was enabled by linking a green  
55 fluorescence protein (GFP) to the N-terminus of the MOR constructs. Two  
56 versions of MOR were expressed, wild-type (exWT) and total phosphorylation  
57 deficient receptors (TPD) where all 11 possible phosphorylation sites on the C-  
58 terminus were mutated to alanine. The results show that both receptors activate a  
59 hyperpolarizing potassium current. There was no significant difference in the  
60 kinetics of activation between WT, exWT, and TPDs. Thus acute activation of  
61 virally expressed MORs was not significantly different from endogenous  
62 receptors. There was however a near complete loss of desensitization,  
63 internalization, and long-term tolerance in neurons expressing TPD receptors.  
64 This study demonstrates a key role of phosphorylation in the both acute- and  
65 long-term actions of opioids on single neurons.

66

## 67 **Results**

### 68 MOR Knockout

69 Recordings from LC neurons in brain slices from the MOR knockout animal  
70 confirmed that there was no current or hyperpolarization induced by opioids with  
71 no detectable difference in the activation of alpha-2-adrenoceptors, orphanin FQ,  
72 or M<sub>3</sub>-muscarine receptors (Figure 1, S1).

73

74 MOR expression

75 Microinjections of adeno-associated virus type 2 containing either the exWT or  
76 TPD receptors were made bilaterally into the LC and after 2-4 weeks the GFP  
77 tagged MORs were visualized with an Olympus macroview microscope (Figure  
78 2A). Images obtained with a 2-photon microscope showed green fluorescence on  
79 the plasma membrane and in the cytoplasm of LC neurons. Plasma membrane  
80 receptors were selectively targeted and labeled using an anti-GFP nanobody  
81 conjugated to Alexa594 dye (Figure 2B-D). There was no labeling of cells from  
82 animals that did not express GFP tagged MORs (Figure 2E,F).

83

84 Electrophysiology of the virally expressed receptors

85 Recordings were made from slices from animals 2-4 weeks following viral  
86 microinjection. Whole-cell voltage clamp or intracellular membrane potential  
87 recordings were made from LC neurons. In each case, application of  
88 [ $\text{Met}^5$ ]enkephalin (ME, 300 nM, an EC<sub>50</sub> concentration in slices from wild type  
89 animals) was used as an estimate of the level of receptor expression. Cells where  
90 the outward current or hyperpolarization induced by this application was either  
91 very large or small were not included in the study.

92 The kinetics of receptor-dependent activation of G protein-gated inwardly  
93 rectifying potassium (GIRK) conductance was examined with the photolysis of  
94 caged-enkephalin (CYLE) using whole-cell recordings in the voltage clamp  
95 configuration (Figure 3). The rate of activation (10-90%, exWT  $238 \pm 33$  ms, n=9,  
96 TPD  $265 \pm 39$  ms, n=19) and the time to the peak of the outward current (exWT  
97  $1.78 \pm 0.12$  s, n=12, TPD  $2.05 \pm 0.20$ , n=18) were the same between exWT and TPD  
98 and similar to those from experiments made from cells expressing wild type  
99 receptors (Figure 3). Likewise the return to baseline following photolysis of the  
100 caged antagonist naloxone (CNV-Nal) in the presence of ME (1  $\mu$ M) was not  
101 different in recordings made from the two receptors (exWT  $1.57 \pm 0.08$  s, n=7,  
102 TPD  $1.53 \pm 0.15$ , n=6, p>0.05). When the high affinity agonist endomorphin-1

103 (100 nM) was used, the time constant of CNV-Nal-induced inactivation in exWT  
104 receptors ( $4.06 \pm 0.41$  s,  $n=8$ ) was not significantly different from that measured  
105 with TPD receptors ( $5.37 \pm 0.59$  s,  $n=10$ ,  $p>0.05$ ). The current amplitudes induced  
106 by endomorphin-1 (290 $\pm$ 37 pA in exWT and 255 $\pm$ 44 pA in TPD) were also  
107 similar ( $p>0.05$ ). Thus, in spite of the multiple mutations along the C-terminus  
108 and the presence of GFP at the N-terminus, the acute signaling of virally  
109 expressed TPD and exWT receptors was not significantly different compared to  
110 receptors from wild type animals.

111

## 112 Desensitization

113 Acute receptor desensitization was compared in slices from animals injected with  
114 either exWT or TPD receptors. Two measures of desensitization were made, the  
115 decrease in the peak (hyperpolarization for intracellular recordings or current for  
116 whole-cell recordings) during the application of a saturating concentration of ME  
117 ( $30 \mu\text{M}$ , 10 min) and the relative decrease in response to an EC<sub>50</sub> concentration  
118 of ME (300 nM) following the washout of the saturating concentration of ME  
119 (Figure 4, S4). The results from experiments with exWT receptors were similar to  
120 results from wild type animals that have been published previously. During the  
121 application of ME ( $30 \mu\text{M}$ ) the membrane potential hyperpolarization measured  
122 with intracellular recording declined to  $75 \pm 5\%$  of the peak ( $n=6$ ). The current  
123 measured under voltage clamp with whole-cell recording declined to  $54 \pm 4\%$  of  
124 the peak ( $n=12$ ). Following the washout of saturating ME ( $30 \mu\text{M}$ ), the  
125 hyperpolarization induced by EC<sub>50</sub> ME (300 nM) was reduced to  $30 \pm 2\%$  ( $n=5$ )  
126 and the current to  $23 \pm 5\%$  ( $n=10$ ) of the pre-desensitization response. Following a  
127 20-30 min wash of ME ( $30 \mu\text{M}$ ) the application of ME (300 nM) approached the  
128 pre-desensitization control with whole cell voltage clamp or intracellular  
129 recordings.

130 The results obtained with the TPD receptors were significantly different. With  
131 intracellular recordings, the hyperpolarization was reduced to  $94 \pm 1\%$  ( $n=7$ ,  
132  $p=0.0003$ ) of the peak and the current declined to  $80 \pm 2\%$  of the peak ( $n=13$ ,

133 p=0.003) in whole cell recordings. Likewise there was only a small decrease in  
134 the response to ME (300 nM) following washout of the saturating concentration  
135 of ME (76±4%, n=5, p=0.0001 in intracellular recording and 81±9% of pre-  
136 desensitization, n=11, p=0.0005 in voltage clamp). Thus by two measures  
137 obtained under two recording conditions, acute desensitization was markedly  
138 reduced in neurons expressing TPD receptors.

139

140 Protein kinase C dependent desensitization

141 MOR desensitization induced by protein kinase C (PKC) has been proposed to be  
142 the result of phosphorylation at S363, T370 or S/T356-357 (Wang et al., 2002;  
143 Feng et al., 2011; Chen et al., 2013; Illing et al., 2014). In previous work using  
144 wild type animals, receptor desensitization was augmented by manipulations that  
145 increased the activity of PKC. The PKC activators, phorbol 12,13-dibutyrate and  
146 phorbol 12-myristate 13-acetate increased the decline from the peak  
147 hyperpolarization during the application of ME (30  $\mu$ M, 10 min) and caused a  
148 small reduction of the hyperpolarization induced by ME (300 nM). Muscarine,  
149 thought to activate PKC by a Gq-dependent mechanism, also induced a large  
150 increase in apparent desensitization (Arttamangkul et al., 2015). In intracellular  
151 recordings from both exWT and TPD receptors, muscarine facilitated the  
152 desensitization induced by ME (30  $\mu$ M, Figure 5). In the presence of muscarine,  
153 the initial amplitude of the hyperpolarization induced by ME (300 nM) decreased  
154 by 43±8% in experiments from exWT, n=5 and by 49±8% from TPD, n=6. The  
155 decline from the peak hyperpolarization induced by ME (30  $\mu$ M, 10 min) was also  
156 facilitated (Figure 5). Although the decline from the peak in experiments  
157 examining the TPD receptors was small, it was over double that measured in the  
158 absence of muscarine (6±1%, n=7 vs. 15±2% in muscarine, n=6, p=0.0009,  
159 unpaired two tailed T-test). Likewise, in whole-cell voltage clamp experiments,  
160 the current amplitude evoked by photolysis of CYLE was significantly decreased  
161 by muscarine and returned to baseline following the application of the  
162 muscarinic antagonist scopolamine (Figure S5). Thus the presumed activation of

163 PKC induced by muscarine acts by a mechanism that is independent of  
164 phosphorylation of the C-terminal of MOR.

165

166 Receptor trafficking – acutely and following chronic morphine treatment  
167 Receptor internalization was studied by immuno-labeling the extracellular N-  
168 terminal GFP of plasma membrane-associated exWT and TPD receptors. Living  
169 slices were incubated in an anti-GFP nanobody-Alexa594 for 30-45 min, placed  
170 in a superfusion chamber and visualized with 2-photon microscopy (Figure 6).  
171 Labeled receptors were imaged before the application of a saturating  
172 concentration of ME (30  $\mu$ M, 10 min) and at the end of the 10 min application.  
173 Similar to a previous study in mouse LC neurons (Arttamangkul et al., 2008),  
174 this treatment induced the internalization of exWT receptors (Figure 6A top).  
175 When TPD receptors were examined using the same treatment protocol there was  
176 no detectable internalization (Figure 6A bottom). Thus, ME induced  
177 internalization of TPD receptors was completely disrupted (exWT receptor  
178 internalization was  $38\pm3\%$  of the total fluorescence, n=7; internalization of the  
179 TPD was  $10\pm5\%$  of the total fluorescence, n=6, p=0.0004).  
180 The development of long-term tolerance induced by chronic morphine treatment  
181 after expression of exWT and TPD receptors was examined next. A previous study  
182 in mouse LC found that the recycling of Flag-MORs was increased after chronic  
183 morphine treatment in the arrestin3 knockout animals (Quillinan et al., 2011).  
184 One possibility is that chronic morphine treatment may result in the modulation  
185 the trafficking pathway of expressed exWT and TPD receptors. Animals were  
186 microinjected with virus to express either exWT or TPD and after 7-10 days  
187 treated chronically with morphine (80 mg/kg/day) using osmotic mini pumps.  
188 After 6 or 7 days brain slices were prepared in morphine-free solutions and slices  
189 were prepared for 2-photon imaging. As expected, exWT receptors were  
190 internalized in slices from morphine treated animals ( $49\pm6\%$ , n=4, Figure 6 B  
191 top). There was however, no internalization of TPD receptors in slices from  
192 morphine treated animals (n=4, Figure 6B bottom). Thus the inability to induce

193 internalization of TPD receptors was maintained following chronic morphine  
194 treatment.

195

196 Tolerance following chronic morphine treatment

197 In whole-cell voltage clamp experiments using slices from morphine treated  
198 animals that expressed exWT receptors, a saturating concentration of ME (30  
199  $\mu$ M) resulted in an outward current that peaked and declined to  $41\pm2\%$  (n=8) of  
200 the peak. The current induced by a subsequent application of ME (300 nM) was  
201 significantly depressed relative to the control (Figure 7B). Unlike the results  
202 obtained in slices from untreated animals, the current induced by ME (300 nM)  
203 never recovered completely over a period of 20-30 min after washout of the  
204 saturating concentration. Thus as has been reported previously in experiments  
205 using wild type animals that were chronically treated with morphine,  
206 desensitization was augmented and the recovery from desensitization was  
207 reduced.

208 In experiments from morphine treated animals expressing the TPD receptor,  
209 there was no significant change in any measure of opioid action. The decline from  
210 the peak current induced by a saturating concentration of ME (30  $\mu$ M 10 min)  
211 was  $83\pm4\%$  in TPD (n=8) and not different from experiments in slices taken from  
212 untreated animals ( $80\pm2\%$ , n=13,  $p>0.05$ , unpaired T-test). The current induced  
213 by ME (300 nM) following washout of the ME (30  $\mu$ M) solution was also not  
214 different from slices of untreated animals (Figure 7C).

215 Finally, the initial rise in current induced by photolysis of CYLE was not different  
216 in slices from untreated and morphine treated animals (10-90% rise time of the  
217 first flash, untreated exWT  $255\pm35$  ms (n=10), TPD  $219\pm32$  ms (n=14); morphine  
218 treated exWT  $201\pm21$  ms (n=10), TPD  $211\pm23$  (n=10). Thus the rising phase of  
219 the current was not changed following chronic morphine treatment. Another  
220 measure of desensitization was examined in slices from morphine treated  
221 animals using photolysis of caged-enkephalin (Figure 8). The peak current and  
222 10-90% rise time was measured in response to repeated 10 ms flashes before and

223 after a longer 100 ms flash. In experiments from exWT expressing cells the  
224 amplitude of the current declined significantly by the 5<sup>th</sup> flash. Following the long  
225 flash, there was a step decrease in the peak current measured in the exWT  
226 receptors (Figure 8C). Likewise the rise time was significantly slowed (Figure  
227 8D). In contrast, the long flash did not alter the peak amplitude or activation rate  
228 of the 10 ms flash-induced currents in recordings from cells expressing TPD  
229 receptors. Thus, the normalized peak currents and activation rates following the  
230 long flash were significantly different between exWT and TPD receptors further  
231 indicating that TPD receptors display little to no desensitization even in slices  
232 from morphine treated animals.

233

## 234 **Discussion**

235 The acute activation, desensitization, endocytosis and the development of  
236 tolerance to opioids were characterized in locus coeruleus neurons from a MOR  
237 knockout rat following the viral expression of exWT and TPD MORs. The results  
238 with the exWT receptors in the knockout animal were similar to those found in  
239 wild type animals. The activation kinetics of TPD receptors was also the same as  
240 both virally expressed and endogenous WT receptors. This study demonstrates  
241 that the elimination of phosphorylation of sites along the C-terminal of the MOR  
242 largely eliminates acute desensitization and the development of long-term  
243 cellular tolerance to morphine. The results also indicate that with the expression  
244 of receptors specifically in the locus coeruleus the development of tolerance is cell  
245 autonomous, independent of receptor activation in other areas of the CNS.

246

### 247 Desensitization and internalization

248 MOR desensitization and internalization are not closely linked. The strongest  
249 evidence is based on experiments using mutation of the STANT sequence.  
250 Although mutations in the STANT sequence resulted in a significant decrease in  
251 internalization, acute desensitization was little changed (Lau et al., 2011, Just et  
252 al., 2013; Birdsong et al., 2015). The conclusion was that acute desensitization

253 precedes internalization and the two processes are mechanistically distinct. The  
254 same conclusion was reached in experiments in cultured locus coeruleus neurons  
255 from a transgenic mouse that expressed soluble GFP under the control of the  
256 tyrosine hydroxylase promotor (TH-GFP). Internalization of the endogenous  
257 MORs measured with the use of a fluorescent peptide, dermorphin-Alexa594,  
258 was blocked by concanavalin A and yet desensitization and the recovery from  
259 desensitization measured electrophysiologically were not changed (Arattamangkul  
260 et al., 2006). The sequence beginning at T354 and ending at T357 (TSST) was  
261 also efficiently phosphorylated following the application of potent opioid agonists  
262 (Lau et al., 2011). An alanine-mutant of C-terminal phosphorylation sites  
263 excluding TSST and T394 (6S/T-A sites) prevented receptor endocytosis while  
264 desensitization remained unchanged (Yousuf et al., 2015). It was not until the  
265 TSST sequence along with the STANT sequence or all phosphosites on the C  
266 terminus were mutated to alanine that there was a large decrease in the degree of  
267 acute desensitization (Birdsong et al., 2015, Yousuf et al., 2015). Similar results  
268 were shown in this study with viral expressed TPD in MOR knockout rats. Thus it  
269 is clear that although acute desensitization and internalization of MOR are  
270 dependent on phosphorylation, the two processes involve mechanisms that can  
271 be distinguished by the degree of phosphorylation of the C-terminal tail.

272

273 The heterologous desensitization induced by muscarinic receptor activation was  
274 not blocked after mutations of C-terminal phosphorylation sites. Activation of  
275 muscarinic receptors can increase PKC activity that is thought to underlie  
276 heterologous desensitization of MORs (Bailey et al., 2004). The muscarine-  
277 induced decrease in activation of potassium conductance in slices expressing the  
278 TPD was similar to results obtained in slices from wild type animals (Shen &  
279 North, 1992; Fiorillo & Williams, 1996). The results may be interpreted in two  
280 ways. One is that the facilitation of MOR desensitization by PKC results from  
281 phosphorylation of intracellular loops of MOR and not at the carboxy tail (Chen  
282 et al., 2013). It is also possible that phosphorylation of other signaling proteins  
283 results in the inhibition (Chu et al., 2010). It has been shown that activation of

284 muscarinic receptor alters the trafficking of MOR heterologous expressed in  
285 HEK293 cells (Lopez-Gimenez et al., 2017), however a previous trafficking study  
286 examining FLAG-MORs in the mouse locus coeruleus found that muscarine  
287 caused no change in internalization (Arttamangkul et al., 2015).

288

289 Is the TPD a G protein biased receptor?

290 Depending on the agonist, MORs can activate differential downstream processes.  
291 A number of biased agonists have been described recently (Siuda et al., 2017). G-  
292 protein biased agonists have reduced ability to recruit arrestin while maintaining  
293 signaling through G proteins. Mutations in the C-terminus of MORs have a  
294 significant impact on arrestin signaling. Mutations of even one phosphorylation  
295 site at S375 and/or the STANT sequence in the C-terminus resulted in a  
296 significant reduction in the association with arrestin and the induction of  
297 internalization (Lau et al., 2011). The STANT mutant MOR was functional as  
298 measured by adenylyl cyclase (Leu et al., 2011) and activation of potassium  
299 conductance (Birdsong et al., 2015) assays. Mutations of all phosphorylation sites  
300 on the C-terminus (TPD) eliminated endocytosis induced by highly efficacious  
301 agonists such as DAMGO, etonitazene and fentanyl in HEK293 cells (Just et al.,  
302 2013) as well as ME in LC neurons (present study). Given these observations, the  
303 TPD receptor could be considered to function almost exclusively through a G  
304 protein-dependent process.

305

306 Cellular tolerance and homeostatic mechanisms

307 One robust measure of tolerance in the LC is a decrease in the recovery from  
308 acute desensitization in slices from morphine treated animals (Dang & Williams,  
309 2004; Quillinan et al, 2011; Levitt & Williams, 2012). In experiments from slices  
310 expressing TPD receptors, chronic morphine treatment had no effect. There are  
311 two possible conclusions that follow this observation. First, the near complete  
312 block of desensitization alone results in reduced tolerance. This however requires  
313 further investigation using a longer duration of morphine treatment. It is possible

314 that tolerance may develop slower. It is also possible that compensatory  
315 homeostatic mechanisms due to continuous signaling may develop from the  
316 longer-term chronic treatment. The second conclusion centers on the G protein  
317 biased nature of this receptor and the elimination of arrestin binding leading to  
318 internalization. It may be that the activation of the arrestin pathway is a key step  
319 in the development of long-term tolerance. Studies using arrestin3-null mice  
320 show that cellular tolerance is attenuated (Quillinan et al., 2011; Dang et al., 2011,  
321 Connor et al., 2015). This could be the result of MOR trafficking because while  
322 the internalization of MORs in these animals was normal, receptor recycling was  
323 faster after chronic morphine treatment (Quillinan et al., 2011). However,  
324 interpretation of these studies is difficult given that only one isoform of arrestin  
325 was knocked out. Experiments expressing phosphorylation mutants in the C-  
326 terminus in the MOR knockout rat could begin to address the role of  
327 internalization in the development of cellular tolerance.

328

329 Summary

330 The present work addresses one mechanism that underlies the development of  
331 long-term tolerance to morphine. Phosphorylation of the C-terminal of the MOR  
332 has been shown to be a key step in the mechanism of acute desensitization.  
333 Elimination of phosphorylation sites on the C-terminal rendered MORs resistant  
334 to cellular measures of long-term tolerance induced by morphine. One conclusion  
335 is that desensitization and/or internalization of MORs is necessary for the  
336 development of cellular tolerance to opioids. Although there were no obvious  
337 change in cellular excitability, it could be that continued signaling through the  
338 phosphorylation deficient receptors result in downstream homeostatic  
339 mechanisms that counteract the lack of cellular tolerance and may well increase  
340 signs of withdrawal.

341

341

342 **Materials and Methods**

343 *Drugs* - Morphine sulfate and morphine alkaloid were obtained from the  
344 National Institute on Drug Abuse (NIDA), Neuroscience Center (Bethesda, MD).  
345 Naloxone was purchased from Abcam (Cambridge, MA), MK-801, from Hello Bio  
346 (Princeton, NJ), UK14304 tartrate, from Tocris (Bio-Techne Corp. Minneapolis,  
347 MN). Potassium methanesulfonate was from Alfa Aesar (Ward Hill, MA). [Met<sup>5</sup>]  
348 enkephalin (ME), endomorphin-1, muscarine, scopolamine, idazoxan and other  
349 reagents were from Sigma (St. Louis, MO). Caged-enkephalin (CYLE) and Caged-  
350 naloxone (CNV-Nal) were a gift from Mathew Banghart.

351 Morphine alkaloid was converted to salt form with 0.1 M HCl and made up  
352 a stock solution in water. The working solution was diluted in artificial  
353 cerebrospinal fluid (ACSF) and applied during incubation or superfusion.  
354 Naloxone, endomorphin-1, muscarine, scopolamine, UK14304 tartrate and  
355 idazoxan were dissolved in water, diluted in ACSF and applied by bath  
356 superfusion. Bath perfusion of ME was with bestatin (10 mM) and thiorphan (1  
357 mM) to limit breakdown of ME.

358

359 *Animals*– All animal experiments were conducted in accordance with the  
360 National Institutes of Health guidelines and with approval from the Institutional  
361 Animal Care and Use Committee of the Oregon Health & Science University  
362 (Portland, OR). Adult (180 – 300 g or 5-6 weeks) male and female Sprague-  
363 Dawley rats were obtained from Charles River Laboratories (Wilmington, MA). A  
364 pair of MOR-knockout Sprague-Dawley rats with ZFN target site  
365 (GCTGTCTGCCACCCAgtaaaGCCCTGGATTTC within exon 2) were generated by  
366 Horizon (St. Louis, MO) and received as F3 generation. The animals were bred  
367 and raised in house for two more generations before used in the experiments. The  
368 gene deletion was confirmed by genotyping using the primer  
369 5'CATATTCACCCCTCTGCACCA3'.

370

371 *Microinjection protocol*-MOR-knockout animals (24-30 days) were anesthetized  
372 with isofluorane (Terrell®, Piramal Clinical Care, Inc., Bethlehem, PA) and  
373 placed in a stereotaxic frame for micro-injection of viral particles containing  
374 adeno associated virus type 2 for the expression of wild type MORs (exWT,  
375 AAV2-CAG-SS-GFP-MOR-WT-WPRE-SV40pA,  $2.06 \times 10^{13}$  vg/ml) and total  
376 phosphorylation deficient MORs (TPD, AAV2-CAG-SS-GFP-MOR-TPD-WPRE-  
377 SV40pA,  $2.21 \times 10^{13}$  vg/ml). Both viruses were obtained from Virovek (Hayward,  
378 CA). Injections of 200 nl at the rate of 0.1  $\mu$ l/min were done bilaterally at  $\pm 1.25$   
379 mm lateral from the midline and -9.72 mm from the bregma at a depth of 6.95  
380 mm from the top of the skull using computer controlled stereotaxic Neurostar  
381 (Kähnerweg, Germany). Experiments were carried out 2-4 weeks following the  
382 injection.

383

384 *Animal treatment protocols*-Rats (5-6 weeks) were treated with morphine sulfate  
385 continuously released from osmotic pumps as described previously (Quillinan et  
386 al., 2011). Osmotic pumps (2ML1, Alzet, Cupertino, CA) were filled with the  
387 required concentration of morphine sulfate in water to deliver 80 mg/kg/day.  
388 Each pump has a 2 ml reservoir that releases 10  $\mu$ l/hour for up to 7 days. Rats  
389 were anesthetized with isoflurane and an incision was made in the mid-scapular  
390 region for subcutaneous implantation of osmotic pumps. Pumps remained in  
391 animals until they were used for experiments 6 or 7 days later.

392

393 *Tissue preparation* – Horizontal slices containing locus coeruleus (LC) neurons  
394 were prepared as described previously (Williams and North, 1984). Briefly, rats  
395 were killed and the brain was removed, blocked and mounted in a vibratome  
396 chamber (VT 1200S, Leica, Nussloch, Germany). Horizontal slices (250-300  $\mu$ m)  
397 were prepared in warm (34°C) artificial cerebrospinal fluid (ACSF, in mM): 126  
398 NaCl, 2.5 KCl, 1.2 MgCl<sub>2</sub>, 2.6 CaCl<sub>2</sub>, 1.2 NaH<sub>2</sub>PO<sub>4</sub>, 11 D-glucose and 21.4  
399 NaHCO<sub>3</sub> and 0.01 (+) MK-801 (equilibrated with 95% O<sub>2</sub>/ 5% CO<sub>2</sub>,  
400 Matheson, Basking Ridge, NJ). Slices were kept in solution with (+)MK-801 for at

401 least 30 min and then stored in glass vials with oxygenated (95% O<sub>2</sub>/ 5% CO<sub>2</sub>)  
402 ACSF at 34°C until used.

403

404 *Electrophysiology* –Slices were hemisected and transferred to the recording  
405 chamber which was superfused with 34°C ACSF at a rate of 1.5 - 2 ml/min.  
406 Whole-cell recordings were made from LC neurons with an Axopatch-1D  
407 amplifier in voltage-clamp mode (V<sub>hold</sub> = -60 mV). Recording pipettes (1.7 – 2.1  
408 MΩ, World Precision Instruments, Saratosa, FL) were filled with internal  
409 solution containing (in mM): 115 potassium methanesulfonate or potassium  
410 methyl sulfate, 20 KCl, 1.5 MgCl<sub>2</sub>, 5 HEPES(K), 10 BAPTA, 2 Mg-ATP, 0.2 Na-  
411 GTP, pH 7.4, 275-280 mOsM. Series resistance was monitored without  
412 compensation and remained < 15 MΩ for inclusion. Data were collected at 400  
413 Hz with PowerLab (Chart version 5.4.2; AD Instruments, Colorado Springs, CO).  
414 Intracellular recordings of membrane potential were made with glass electrodes  
415 (50-80 MΩ, World Precision Instruments, Saratosa, FL,) filled with KCl (2 M)  
416 and an Axoclamp-2A amplifier. Hyperpolarizing current (<20 pA) was used to  
417 prevent spontaneous firing of LC neurons. The depolarization induced by  
418 muscarine was corrected with the addition of more hyperpolarizing current to  
419 inhibit firing. Most drugs were applied by bath superfusion. In some  
420 experiments, [Leu<sup>5</sup>]enkephalin was applied by photolysis of caged-  
421 [Leu<sup>5</sup>]enkephalin (CYLE). A solution containing CYLE (30 μM), bestatin (1 μM)  
422 and thiorphan (10 μM) was recycled for photolysis experiments. In other  
423 experiments naloxone was released from the solution of caged-naloxone (CNV-  
424 Nal, 5 μM) recycled in the presence of agonist (ME 1 μM, or endomorphin-1 100  
425 nM). Photolysis was carried out with a full-field illumination of a 365-nm LED  
426 lamp (Thorlabs, Inc., Newton, NJ) attached to the epifluorescence port.

427

428 *Anti-GFP nanobody expression and purification*-A nanobody recognizing GFP  
429 was obtained from Addgene (Cambridge, MA) and cloned into the pET-22b  
430 vector with N-terminal 8xHis-tag followed by thrombin cleavage site. The lysine

431 at 116 of nanobody was mutated to cysteine for a single dye-labeling site. Protein  
432 expression was conducted in *E-coli* strain BL21 (New England BioLabs, Ipswich,  
433 MA) in Terrific Broth medium. The cell culture was grown to OD<sub>600</sub> 0.7 to 1.0 at  
434 37°C, and protein synthesis was induced by 0.5 mM of isopropyl β-D-1-  
435 thiogalactopyranoside and was fermented at 20°C for 18 h. Cells were harvested  
436 by centrifugation and then lysed in a lysing buffer (in mM): 50 HEPES, 500 NaCl,  
437 5 DL-dithiothreitol, 10 imidazol and 10% glycerol using a sonicator (10 min, 4 s  
438 sonication, 8 s paused, on ice). The debris was eliminated by centrifugation and  
439 the clear lysate was purified using the HisTrap column (GE Healthcare,  
440 Marlborough, PA). The His-tag was removed by adding thrombin protease  
441 (Sigma-Aldrich (St. Louis, MO) in to the protein solution at 1:100 (by mass) and  
442 incubated at 4°C overnight. The protein was further purified by size-exclusive  
443 chromatography (Superdex 200) in Dulbecco's Phosphate Buffered Saline  
444 (Thermo Fisher Scientific, (Waltham, MA). Peak fractions having a single band  
445 by SDS-Page (10-20% gradient) electrophoresis were pooled and concentrated to  
446 ≈0.6mg/ml.

447

448 *Anti-GFP nanobody Alexa594 conjugation*-The site-specific fluorescent labeling  
449 of the cysteine-mutated nanobody was modified from previously described  
450 (Pleiner et al., 2015). A solution containing the nanobody (100 µg) was used for  
451 the conjugation reaction. The solution was mixed with tris-(2-  
452 carboxyethyl)phosphine 15 mM on ice for 10 min. The buffer was exchanged to  
453 labeling buffer using P6 spin-column (BioRad, Hercules, CA). A labeling reaction  
454 was started by adding 1.5-fold of Alexa 594 maleimide (2 µl of 5 µg/µl in  
455 dimethylsulfoxide). The reaction proceeded on ice for 1 h. The conjugated  
456 nanobody was further purified by Superdex 200 in phosphate buffer. The degree  
457 of labeling was determined by measuring OD at 280 and 594 and was close to 1.

458

459 *MOR-GFP Trafficking*-Brain slices (240  $\mu$ m) from the virally injected rats were  
460 prepared as previously described. Slices were visualized with an Olympus  
461 Macroview fluorescent microscope for GFP expression in the LC area and then  
462 incubated in a solution of anti-GFP nanobody Alexa594 (Nb-A594, 10  $\mu$ g/mL, 30-  
463 45 min). Images were captured with an upright microscope (Olympus, Center  
464 Valley, PA.) equipped with a custom-built two-photon apparatus and a 60x water  
465 immersion lens (Olympus LUMFI, NA1.1, Center Valley, PA). The dye was excited  
466 at 810 nm. Data were acquired and collected using Scan Image Software  
467 ((Pologruto et al., 2003). A z-series of 15-20 sections was collected at 1 $\mu$ m  
468 intervals. Drugs were applied by perfusion at the rate of 1 ml/min. All  
469 experiments were done at 35°C. Internalization was calculated as percent of  
470 fluorescence in cytoplasm before and after ME application. The area of interest  
471 obtained by drawing the line along the plasma membrane.

472

473 *Data Analysis* - Analysis was performed using GraphPad Prism 4 software (La  
474 Jolla, CA). Values are presented as mean  $\pm$  SEM. Statistical comparisons were  
475 made using t-test or two-way ANOVA, as appropriate. Comparisons with  $p < 0.05$   
476 were considered significant.

477

478 *Competing Interests* None of the authors have financial or non-financial  
479 competing interests.

480

481

481 **References**

482 Arttamangkul S, Birdsong W, Williams JT (2015) Does PKC activation increase  
483 the homologous desensitization of  $\mu$  opioid receptors? *Br J Pharmacol* **172**: 583-  
484 592.

485 Arttamangkul S, Quillinan N, Low MJ, von Zastrow M, Pintar J, Williams JT  
486 (2008) Differential activation and trafficking of  $\mu$ -opioid receptors in brain slices.  
487 *Mol Pharmacol* **74**:972-979.

488 Arttamangkul S, Torrecilla M, Kobayashi K, Okano H, Williams JT (2006)  
489 Separation of mu-opioid receptor desensitization and internalization:  
490 endogenous receptors in primary neuronal cultures. *J Neurosci* **26**: 4118-4125.

491 Bailey CP, Kelly E, Henderson G (2004). Protein kinase C activation enhance  
492 morphine-induced rapid desensitization of mu-opioid receptors in mature rat  
493 locus ceruleus neurons. *Mol Pharmacol* **66**:1592-1598.

494 Birdsong WT, Arttamangkul S, Bunzow JR, Williams JT (2015) Agonist binding  
495 and desensitization of the  $\mu$ -opioid receptor is modulated by phosphorylation of  
496 the C-terminal tail domain. *Mol Pharmacol* **88**: 816-824.

497 Chen YJ, Oldfield S, Butcher AJ, Tobin AB, Saxena K Gurevich VV, Benovic JL,  
498 Henderson G, Kelly E (2013) Identification of phosphorylation sited in the  
499 COOH-terminal tail of the  $\mu$ -opioid receptor *J Neurochem* **124**, 189-199.

500 Chu J, Zheng H, Zhang Y, Loh HH, Law PY (2010) Agonist-dependent mu-opioid  
501 receptor signaling can lead to heterologous desensitization. *Cell Signal* **22**: 684-  
502 696.

503 Connor M, Bagley EE, Chieng BC, Christie MJ (2015)  $\beta$ -Arrestin-2 knockout  
504 prevents development of cellular  $\mu$ -opioid receptor tolerance but does not affect  
505 opioid-withdrawal-related adaptations in single PAG neurons. *Br J Pharmacol*  
506 **172**: 492-500.

507 Dang VC, Chieng B, Azriel Y, Christie M (2011) Cellular morphine tolerance  
508 produced by  $\beta$  arrestin-2-dependent impairment of  $\mu$ -opioid receptor  
509 resensitization. *J Neurosci* **31**: 7122-7130.

510 Dang VC, Williams JT (2004) Chronic morphine treatment reduces recovery  
511 from opioid desensitization. *J Neurosci* **24**: 7699-7706.

512 Feng B, Li Z, Wang JB (2011) Protein kinase C-mediated phosphorylation of the  
513  $\mu$ -opioid receptor and its effects on receptor signaling. *Mol Pharmacol* **79**: 768-  
514 775.

515 Fiorillo CD, Williams JT (1996) Opioid desensitization: interactions with G-  
516 protein coupled receptors in the locus coeruleus. *J Neurosci* **16**:1479-1485.

517 Illing S, Mann A, Schulz S (2014) Heterologous regulation of agonist-  
518 independent  $\mu$ -opioid receptor phosphorylation by protein kinase C. *Br J  
519 Pharmacol* **171**: 1330-1340.

520 Just S, Illing S, Trester-Zedlitz M, Lau EK, Kotowski SJ, Miess E, Mann A, Doll C,  
521 Trinidad JC, Burlingame AL, von Zastrow M, Schulz S (2013) Differentiation of  
522 opioid drug effects by hierachical multi-site phosphorylation. *Mol Pharmcol* **83**:  
523 633-639.

524 Lau EK, Trester-Zedlitz M, Trinidad JC, Kotowski SJ, Krutchinsky AN,  
525 Burlingame AL, von Zastrow M (2011) Quantitative encoding of the effect of a  
526 partial agonist on individual opioid receptors by multisite phosphorylation and  
527 threshold detection. *Sci Signal* **4**: ra52.

528 Levitt ES, Williams JT (2012) Morphine desensitization and cellular tolerance are  
529 distinguished in rat locus ceruleus neurons. *Mol Pharmacol* **82**: 983-992.

530 Lopez-Gimenez JF, Alvarez-Curto E, Milligan G (2017) M3 muscarinic  
531 acetylcholine receptor facilitates the endocytosis of mu opioid receptor mediated  
532 by morphine independently of the formation of heteromeric complexes. *Cell  
533 Signal* **35**: 208-222.

534 Pleiner T, Bates M, Trakhanov S, Lee CT, Schliep JE, Chug H, Böhning M, Stark  
535 H, Urlaub H, Görlich D (2015) Nanobodies: site-specific labeling for super-  
536 resolution imaging, rapid epitope-mapping and native protein complex isolation.  
537 *Elife* **4**: e11349.

538 Pologruto TA, Sabatini BL, Svoboda K (2003). Scanimage: flexible software for  
539 operating laser scanning microscopes. *Biomed Eng Online* **2**:13.

540 Quillinan N, Lau EK, Virk M, von Zastrow M, Williams JT (2011) Recovery from  
541  $\mu$ -opioid receptor desensitization after chronic treatment with morphine and  
542 methadone. *J Neurosci* **31**: 4434-4443.

543 Shen KZ, North RA (1992) Muscarine increases cation conductance and  
544 decreases potassium conductance in rat locus coeruleus neurons. *J Physiol* **455**:  
545 471-485.

546 Wang HL, Chang WT, Hau PC, Chow YW, Li AH (2002) Identification of two C-  
547 terminal amino acids, Ser(355) and Thr(357), required for short-term  
548 homologous desensitization of mu-opioid receptors. *Biochem Pharmacol* **64**:  
549 257-266.

550 Williams JT, Ingram SL, Henderson G, Chavkin C, von Zastrow M, Schulz S,  
551 Koch T, Evans CJ, Christie MJ (2013) Regulation of  $\mu$ -opioid receptors:  
552 desensitization, phosphorylation, internalization, and tolerance. *Pharmacol Rev*  
553 **65**:223-254.

554 Williams JT, North RA (1984) Opiate-receptor interactions on single locus  
555 coeruleus neurons. *Mol Pharmacol* **26**: 489-497.

556 Yousuf A, Miess E, Sianati S, Du YP, Schulz S, Christie MJ (2015) Role of  
557 phosphorylation sites in desensitization of  $\mu$ -opioid receptor. *Mol Pharmacol* **88**:  
558 825-835.

559

559 **Author contributions**

560 Conceptualization - SA & JTW, Tool building - SA, JRB, XS, Data Curation - SA,  
561 DAH, JTW, Formal Analysis, SA, DAH, JTW, writing-original draft – JTW, draft  
562 editing, SA.

563 **Animals/Key Resources**

564 All experiments were done in accordance with the Institutional Animal Care and  
565 Use Committees (IACUCs) at Oregon Health & Science University (OHSU). A  
566 colony of MOR knockout rats was maintained in house.

567 **Acknowledgements**

568 This work was supported by NIH funding DA08163 (JTW). We thank members  
569 of the Gouaux lab for help in preparing the anti-GFP nanobody and members of  
570 the Williams lab for comments on the work.

571

571

572 Figure legends

573 Figure 1. Locus coeruleus neurons are not sensitive to opioids in the MOR  
574 knockout rat. A, from a MOR knockout animal where the alpha-2-adrenoceptor  
575 agonist, UK14304 (3  $\mu$ M) and OFQ both activate potassium currents whereas ME  
576 (30  $\mu$ M) had no effect. B, from a neuron where the wild type MOR (exWT) was  
577 expressed in the MOR knockout animal. In this recording ME (1  $\mu$ M), morphine  
578 (10  $\mu$ M) as well as UK14304 (3  $\mu$ M) all caused outward currents.

579 Supplement Figure 1. The firing rate of locus coeruleus neurons is not changed by  
580 opioids in recordings from the MOR knockout animal. Examples of recording  
581 with intracellular electrodes from three neurons. Application of ME (30  $\mu$ M) had  
582 no effect on the firing rate however both UK14304 (3  $\mu$ M, A) and OFQ (1  $\mu$ M, B)  
583 inhibited firing and caused a hyperpolarization of the membrane potential. C,  
584 application of muscarine (10  $\mu$ M) increased the firing rate of the LC neuron.

585

586 Figure 2. Microinjection of virus expressing GFP-tagged exWT receptors in the  
587 locus coeruleus of MOR knockout rat. A, low power image of the GFP  
588 fluorescence observed in a horizontal slice containing the LC. B, shows an image  
589 obtained with a 2-photon microscope showing the GFP fluorescence. C, the same  
590 neuron showing the plasma membrane associated receptors following incubation  
591 of the slices with an anti-GFP nanobody conjugated with alexa594. D, the merged  
592 image of the GFP and alexa594 fluorescence. E, a scanning DIC image of a LC  
593 neuron from a knockout animal. F, the same neuron following incubation of the  
594 slice with the anti-GFP nanobody conjugated with alexa594. Scale bar = 10  $\mu$ m.

595

596 Figure 3. The kinetics of activation and inhibition of expressed wild type  
597 receptors (exWT) in LC neurons from the MOR knockout measured with  
598 photolysis of caged enkephalin (CYLE). A, repeated photolysis events (1/2 min)  
599 resulted in rapidly rising outward currents. Right side, the rate of rise was

600 measured as the time it took to go from 10 to 90% of the peak. B, the high affinity  
601 agonist endomorphin 1 (100 nM) was applied along with caged-naloxone (5  $\mu$ M).  
602 At the arrow a 1 s photolysis flash was applied and the decrease in the outward  
603 current was measured. Right side is an expanded time base of the decrease in  
604 outward current and the single exponential fit to that decline.

605

606 Figure 4. Desensitization is largely blocked in experiments carried out in neurons  
607 expressing the TPD. Experiments carried out with intracellular recordings of  
608 membrane potential. A, an example of an experiment with a cell expressing the  
609 exWT receptor. An EC<sub>50</sub> was applied before and following application of a  
610 saturating concentration of ME. The amplitude of the hyperpolarization induced  
611 by ME (30  $\mu$ M) decreased during the 10 min application. The hyperpolarization  
612 induced by ME (300 nM) was reduced and recovered slowly following washout of  
613 ME (30  $\mu$ M). B, the same experiment carried out in neurons that expressed the  
614 TPD receptor. C, summarized results showing the decline in the  
615 hyperpolarization during the application of ME (30  $\mu$ M). There is only a small  
616 decline in experiments carried out with the TPD receptor. D, summarized results  
617 showing the recovery from desensitization. Experiments with neuron in wild type  
618 animal (WT) and the expressed exWT receptors show a slow recovery, whereas  
619 there was little sign of desensitization in the experiments from the TPD receptor.

620

621 Supplement Figure 4. Reduced desensitization of the TPD receptor measured  
622 with whole cell voltage clamp recording. A, shows the outward current induced  
623 by application of different concentrations of ME. In this experiment ME (0.1  $\mu$ M)  
624 was tested before and following the application of ME (30  $\mu$ M, 10 min). The  
625 current induced by ME (30  $\mu$ M) peaked and declined during the 10 min  
626 application and following the washout the current induced by ME (0.1  $\mu$ M) was  
627 reduced and recovered slowly. B, the same experiment carried out with a neuron  
628 expressing the TPD receptor. The decline in the current induced by ME (30  $\mu$ M)

629 over 10 min was smaller than that in the exWT experiment and the decrease in  
630 the current induced by ME (0.3  $\mu$ M) was also largely eliminated.

631

632 Figure 5. Muscarine inhibits ME-induced hyperpolarization and increases  
633 desensitization of WT, exWT and TPD receptors. Recording of membrane  
634 potential made using intracellular electrodes. A, a recording from a neuron in a  
635 slice from a wild type animal. The hyperpolarizations induced by ME (300 nM)  
636 and noradrenline (NA 5  $\mu$ M, plus cocaine 3  $\mu$ M and prazosin 500 nM to prevent  
637 reuptake) were both decreased in the presence of muscarine (10  $\mu$ M). The  
638 hyperpolarization induced by ME (30  $\mu$ M) peaked and declined during the 10  
639 min application. B, the same experiment carried out in a recording from an exWT  
640 receptor. The hyperpolarization induced by ME (300 nM) was reduced and the  
641 decline in the hyperpolarization induced by ME (30  $\mu$ M) was increased in the  
642 presence of muscarine (10  $\mu$ M). C, an experiment with the TPD receptor showing  
643 the lack of decline in the hyperpolarization during the application of ME (30  $\mu$ M).  
644 D, the same experiment carried out in the presence of muscarine (10  $\mu$ M). The  
645 initial hyperpolarization induced by ME (300 nM) is reduced and there is a  
646 greater decline in the hyperpolarization during the application of ME (30  $\mu$ M). E,  
647 summary of the inhibition of the initial hyperpolarization induced by ME and NA  
648 in WT, exWT and TPD receptors, two-tailed paired t-test (\*\* p<0.01,  
649 \*\*\*\*p<0.0001). F, summary of the decline in the hyperpolarization in control and  
650 in the presence of muscarine. The muscarine-induced increase in decline in  
651 experiments from WT and exWT receptors is the same (WT n=15 in control 11 in  
652 muscarine; exWT n=5 in control, 5 in muscarine). There is also a small but  
653 significant increase in the decline found in experiments with the TPD receptor  
654 (n=8 in control, 6 in muscarine, p<0.0001, two way ANOVA, Bonferroni)

655

656 Supplement Figure 5. Whole cell voltage clamp experiment showing the  
657 inhibition of the outward current induced by photolysis of CYLE caused by  
658 muscarine (10  $\mu$ M). A, an example of an experiment. Outward currents were

659 induced before the application of muscarine (10  $\mu$ M) and following the addition  
660 of the muscarinic antagonist, scopolamine (1 M). Muscarine caused an inward  
661 current and the outward current was reversibly decreased. B, the rate of rise of  
662 the current induced by photolysis of CYLE was reduced by muscarine, similar to  
663 that reported following acute desensitization. C, summarized results from  
664 experiments carried out in exWT and TPD receptors. Although desensitization  
665 was blocked in experiments with TPD receptors the inhibition by muscarine was  
666 not changed.

667

668 Figure 6. Receptor trafficking of the TPD is blocked in slices from untreated and  
669 morphine treated animals. Images from exWT (top) and TPD (bottom) showed  
670 receptor distribution before and following application of ME (30  $\mu$ M, 10 min).  
671 The exWT receptors became punctate and moved into the cytoplasm in slices  
672 from untreated (A, top) and morphine treated (B, top) animals. The TPD  
673 receptors did not traffic in slices from untreated (A, bottom) or morphine treated  
674 animals (B, bottom). Scale bar = 10  $\mu$ m.

675

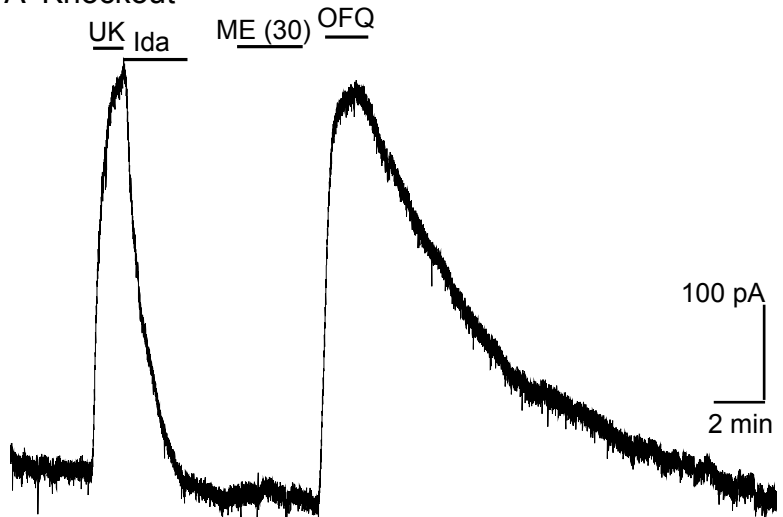
676 Figure 7. There is no sign of long-term tolerance induced in the TPD receptor  
677 following chronic morphine treatment. Whole cell voltage clamp experiments. A,  
678 an example from a morphine treated animal expressing the TPD receptor. There  
679 was a small decline in the current induced by a saturating concentration of ME  
680 (30  $\mu$ M, 10 min) and a small and transient decrease in the current induced by ME  
681 (0.3  $\mu$ M) following the washout of the ME (30  $\mu$ M). B, summary shows the  
682 recovery from desensitization induced by ME (30  $\mu$ M, 10 min) in exWT. There is  
683 significantly less recovery from desensitization seen in experiments from  
684 morphine treated animals than untreated controls with the exWT receptor  
685 ( $p=0.0001$ , two way ANOVA, Bonferroni). C, summarized results from untreated  
686 and the morphine treated animals expressing the TPD receptors. There was a  
687 small (not significant) decrease in the ME (0.3  $\mu$ M) current immediately after the  
688 ME (30  $\mu$ M) treatment in experiments from animals expressing the TPD receptor

689 that did not change with time. There were no difference between the recoveries  
690 from the untreated and morphine treated animals at any points ( $P>0.3$ , ANOVA  
691 Bonferroni).

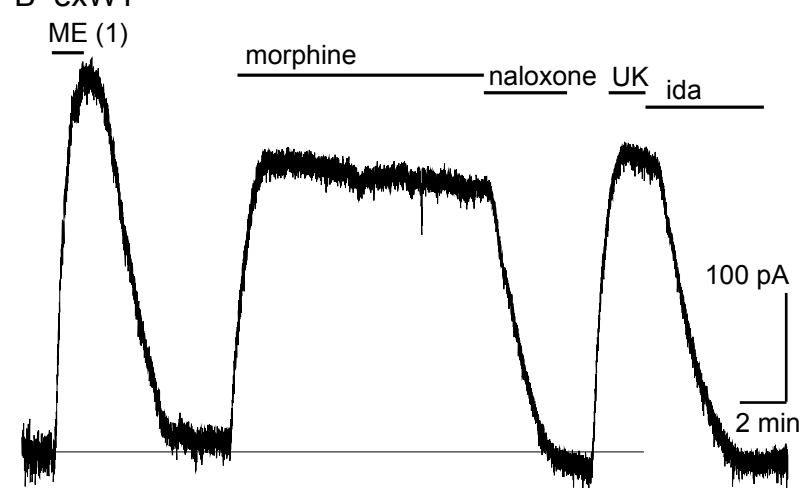
692

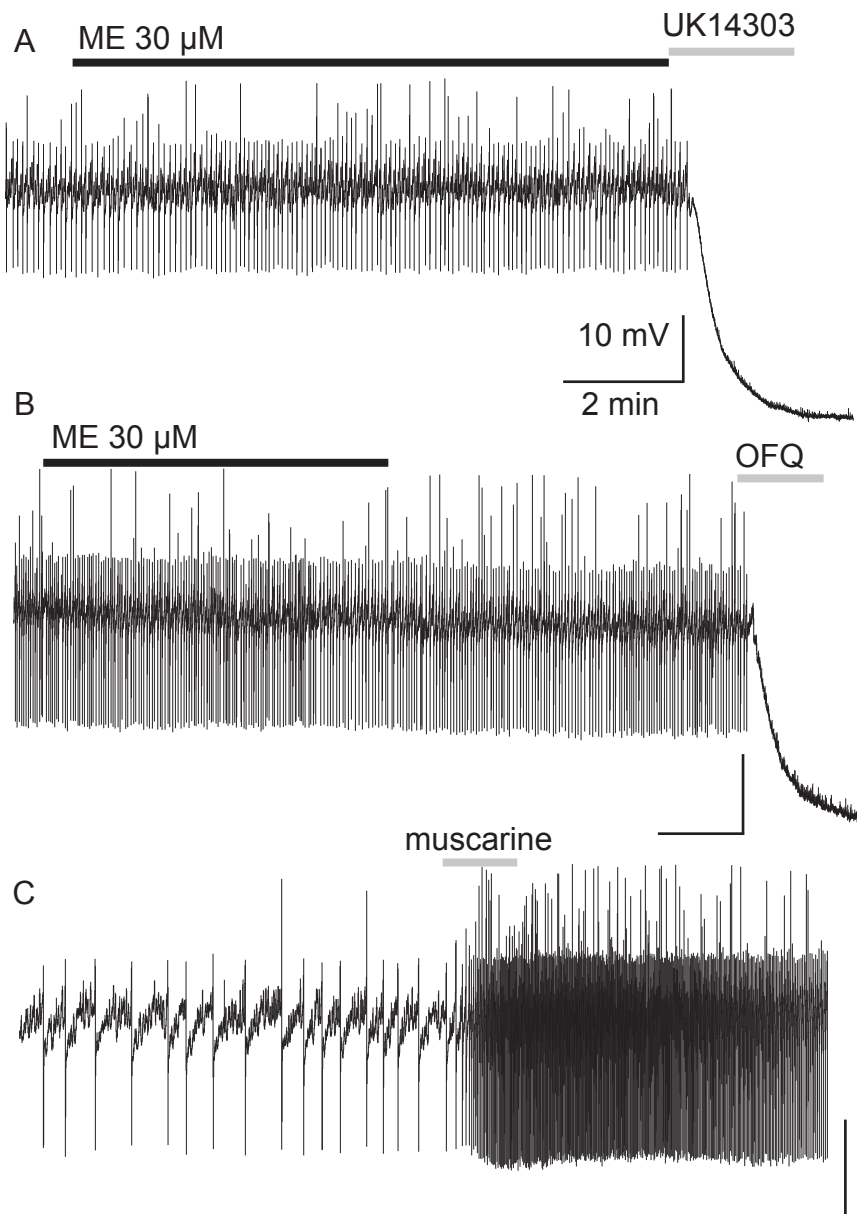
693 Figure 8. Measures of acute desensitization induced by photolysis of caged  
694 enkephalin (CYLE) in slices from morphine treated animals. Whole cell voltage  
695 clamp recordings were made from neurons expressing the TPD or exWT  
696 receptors. A, exWT and B, TPD are example experiments where photolysis of  
697 CYLE was carried out every 2 min. The initial duration of the flash was 10 ms,  
698 after 5 flashes the duration of the flash was increased to 100 ms and subsequent  
699 flashes were 10 ms. C, shows summarized results of the amplitude of the outward  
700 currents. In recordings from exWT receptors the amplitude of the current induce  
701 by the 10 ms flash decreased steadily ( $p=0.002$ ). Increasing the duration of the  
702 flash increased the peak current and the amplitude of the subsequent currents  
703 induced by 10 ms flashes was decreased ( $p<0.0001$ ). The current induced by the  
704 10 ms flashes in experiments from the TPD receptor were not changed ( $p>0.3$ ).  
705 The decline in current in the exWT receptors is significantly different than in the  
706 TPD receptors ( $p=0.0001$ , ANOVA, Dunnett test). D, Summary of the rise time  
707 (10-90%) of the outward current in exWT and TPD receptors. The rise increased  
708 steadily in exWT receptors ( $p=0.005$ ). The rise time was no significant change in  
709 the rise time in recordings from the TPD receptors ( $p>0.05$ ).

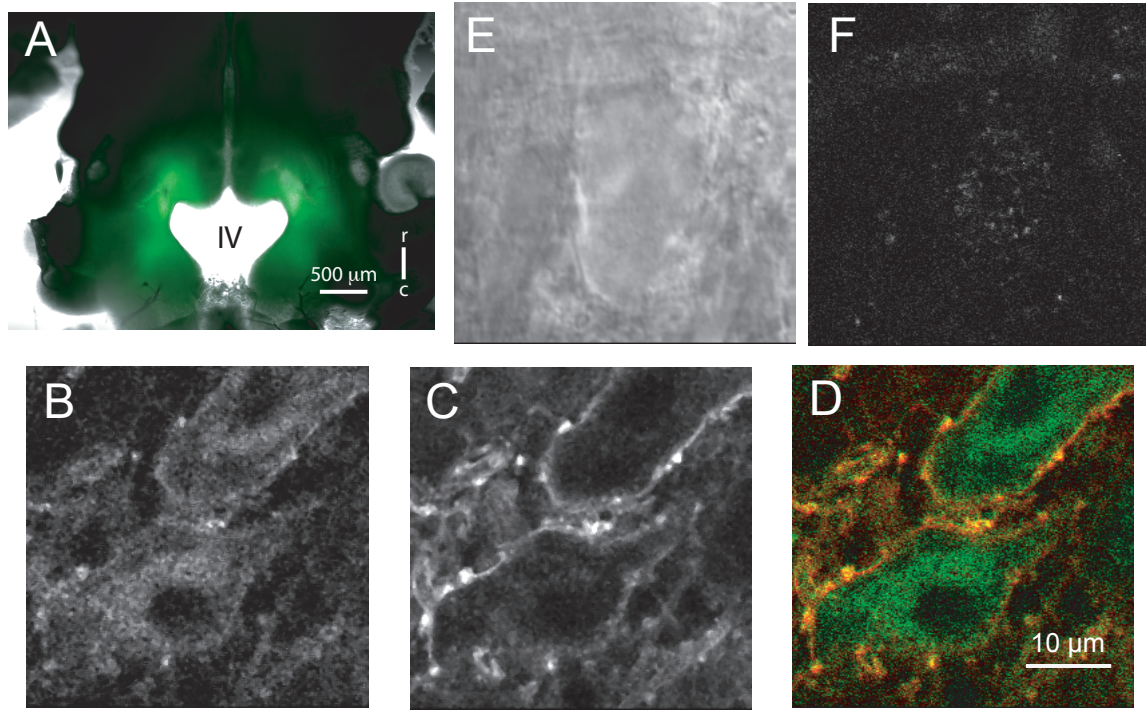
**A Knockout**



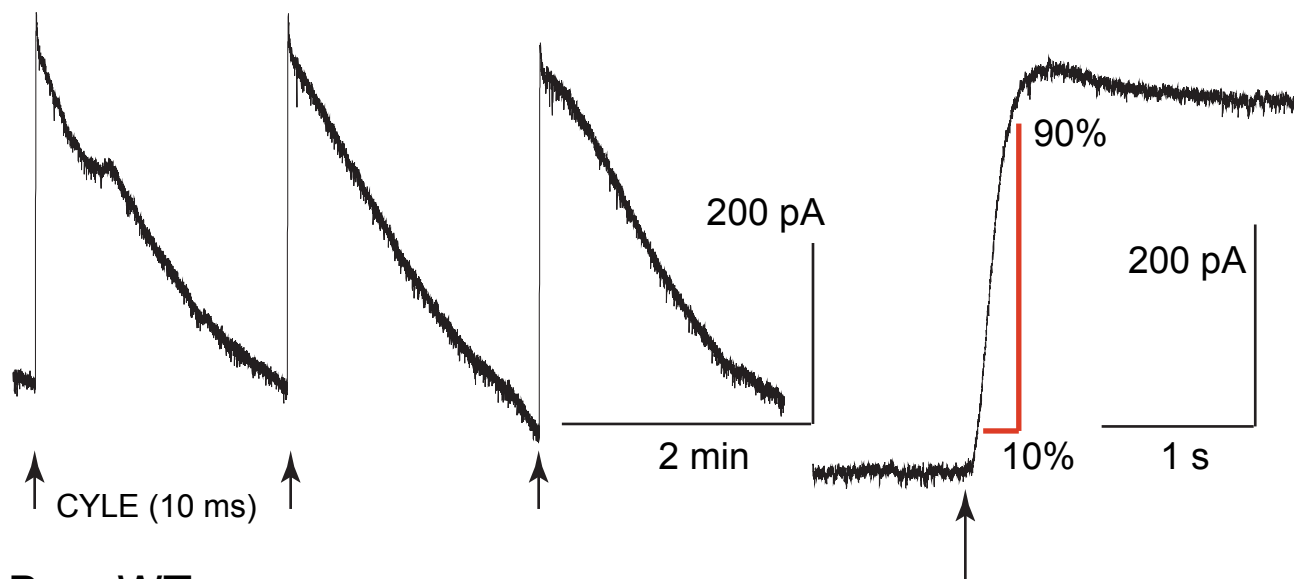
**B exWT**





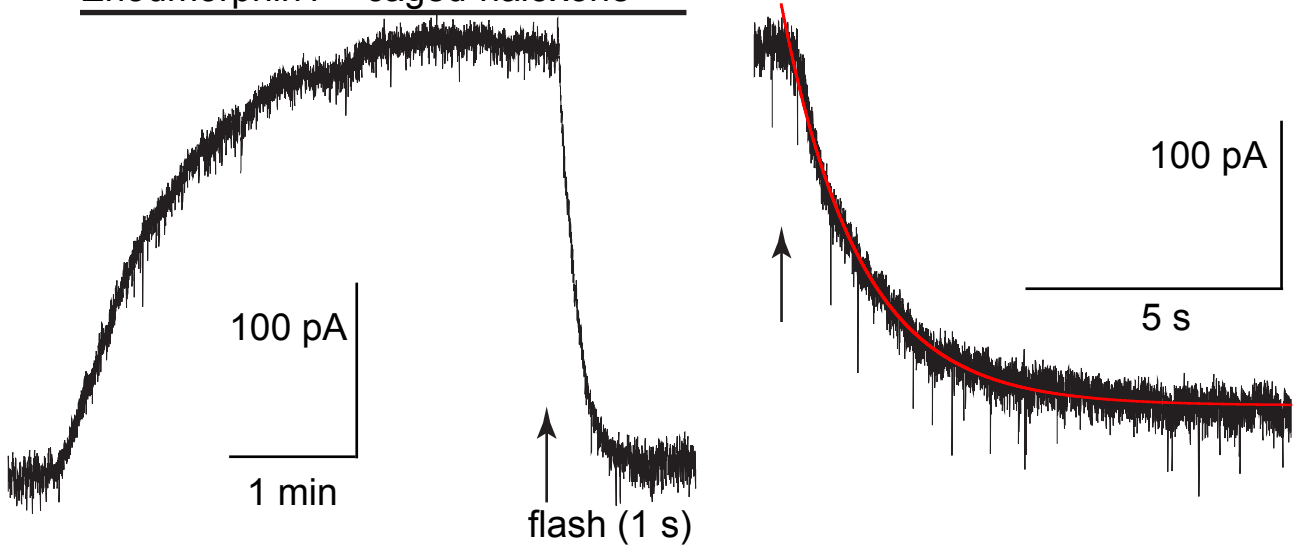


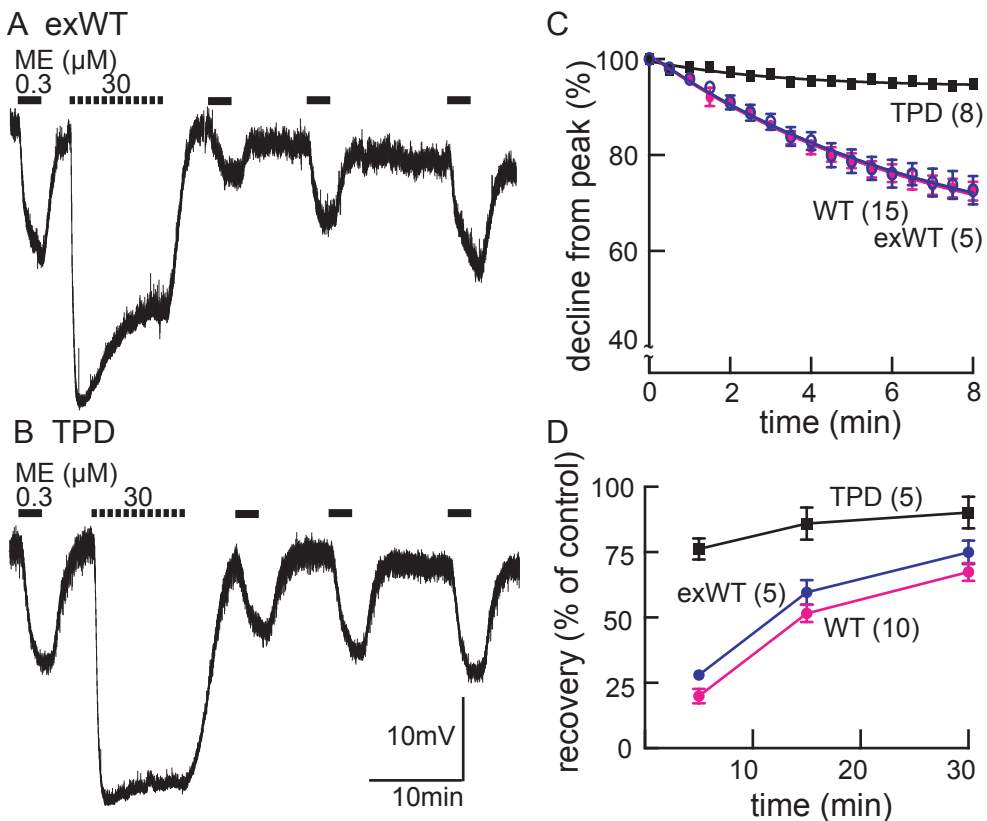
**A exWT**



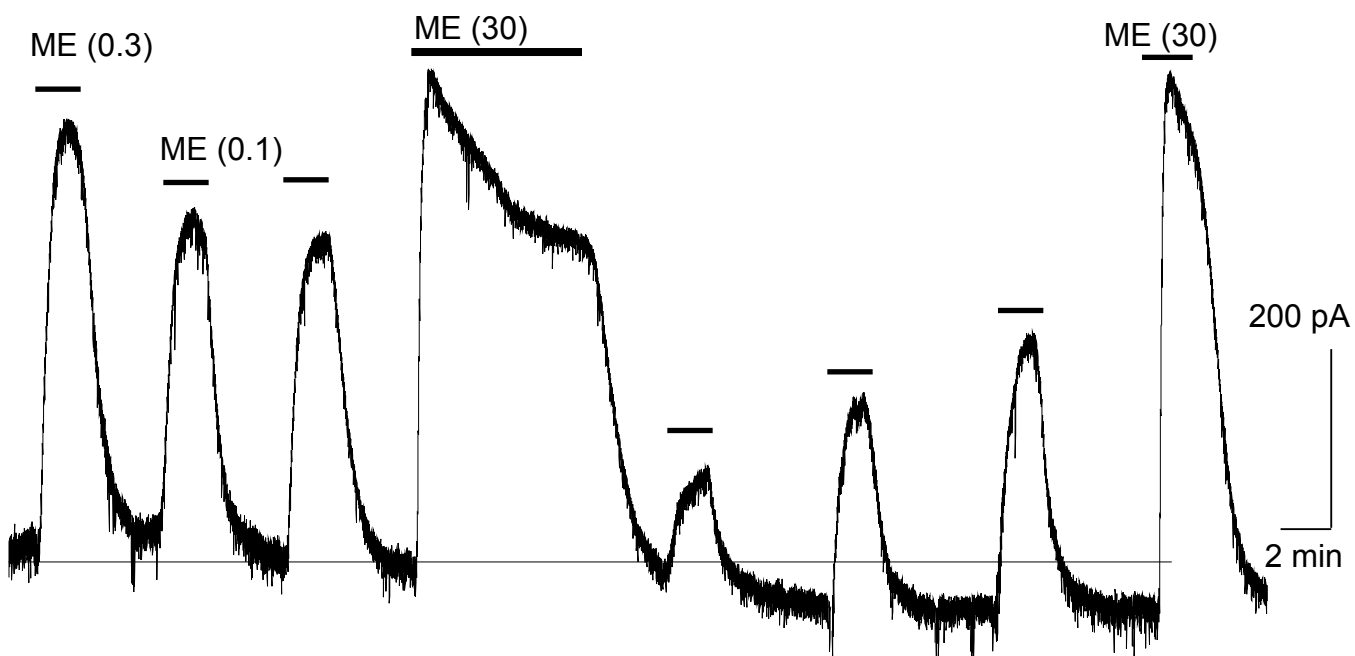
**B exWT**

Enodmorphin1 + caged-naloxone

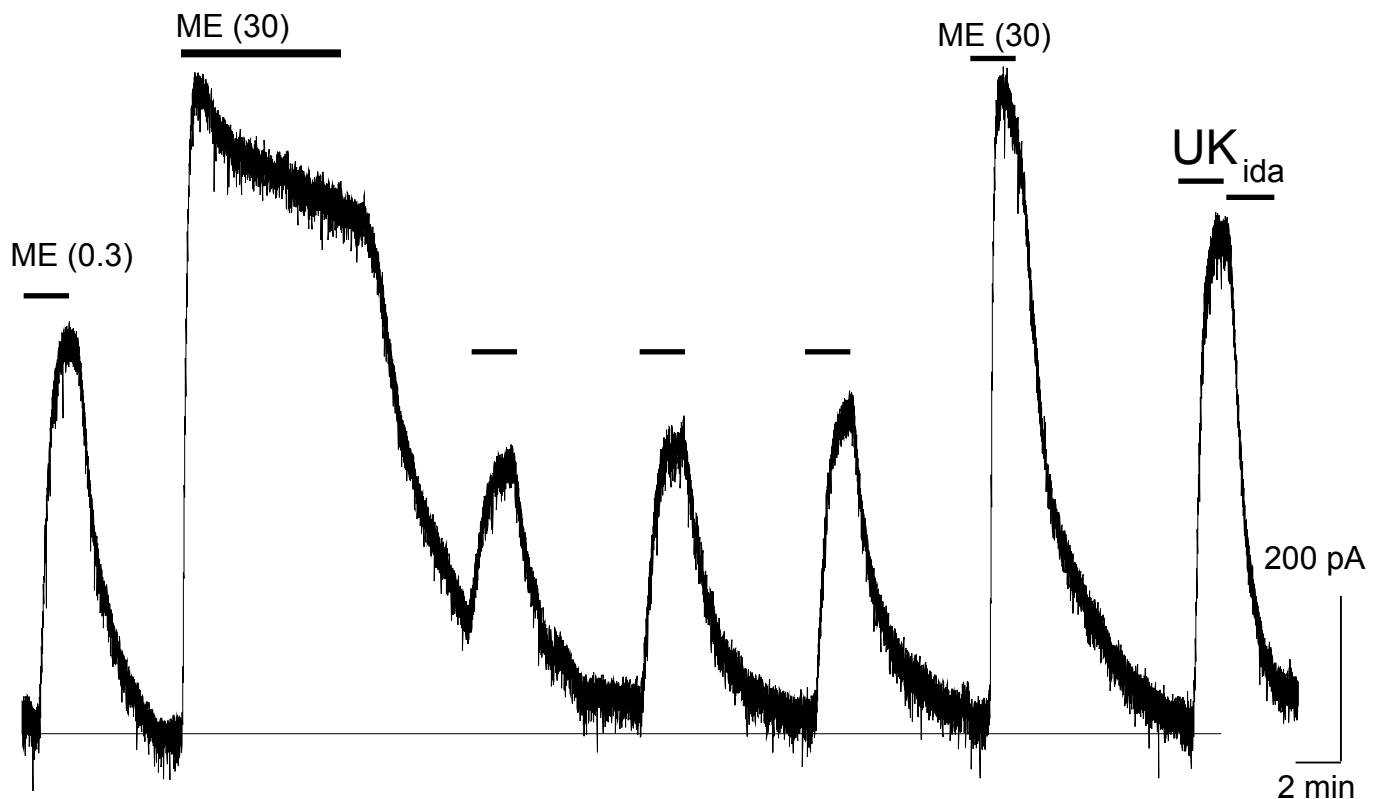


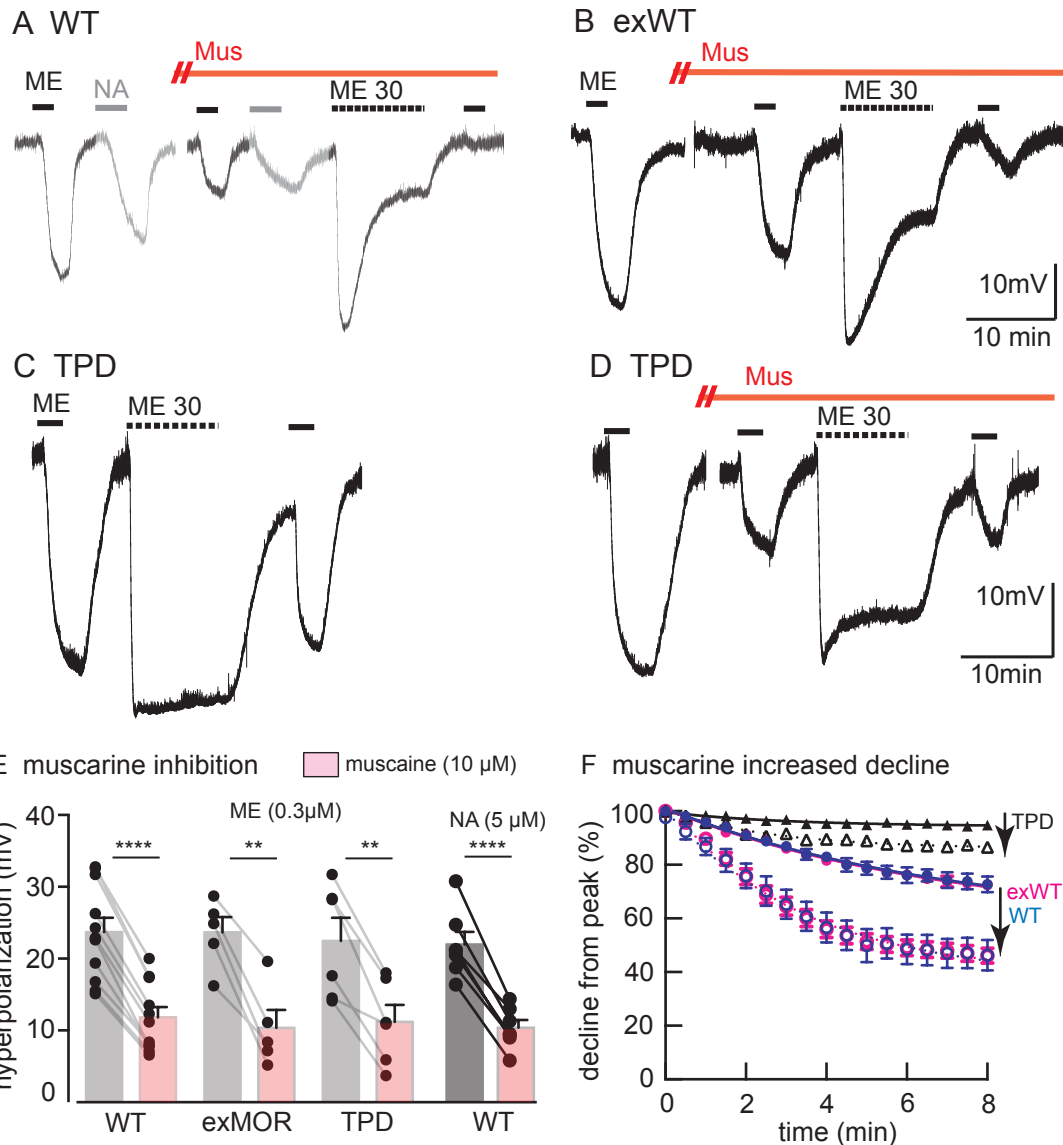


## A exWT

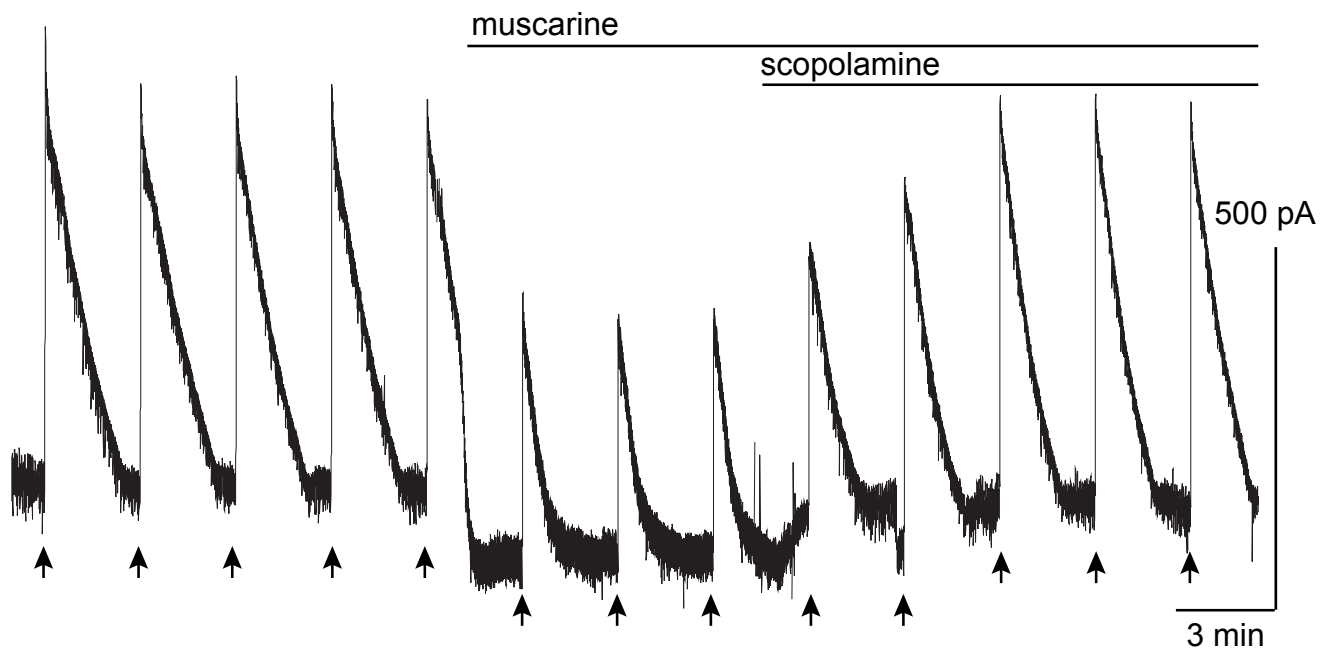


## B TPD

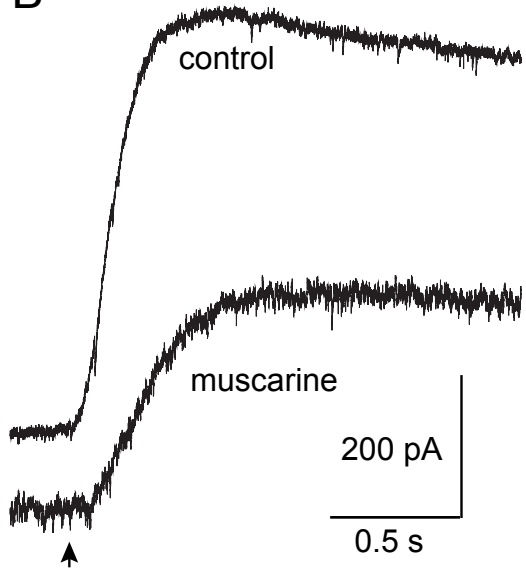




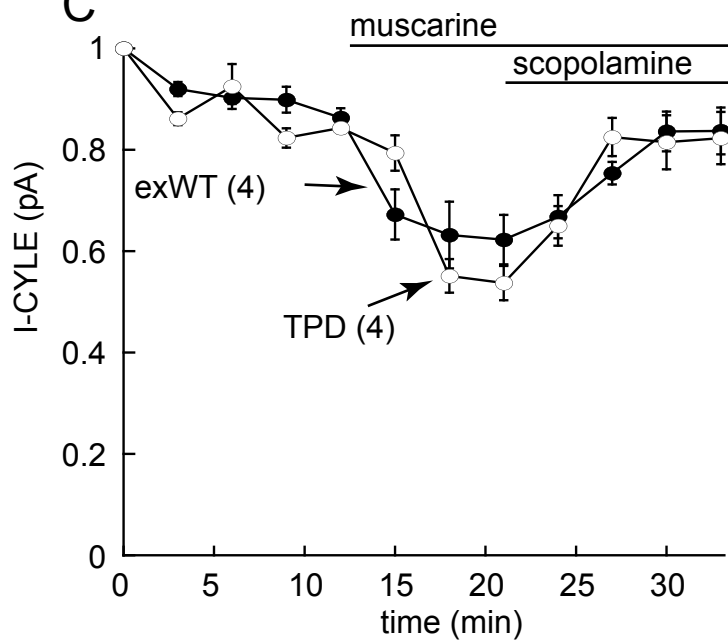
A



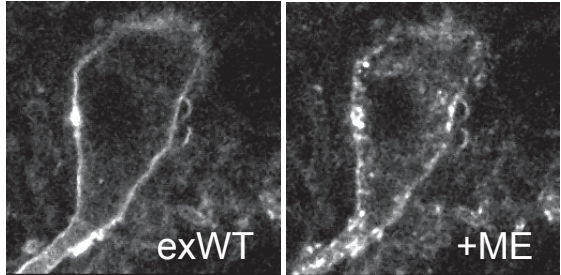
B



C



A untreated



B morphine treated

